

# Mapping regolith strength for bauxite mine rehabilitation using instrumented bulldozers

Faron C. Mengler, Bob Gilkes and Geoff Kew

Centre for Land Rehabilitation, School of Earth and Geographical Sciences, The University of Western Australia,  
Mail Delivery Point M087 35 Stirling Highway, Crawley, Western Australia 6009, AUSTRALIA.  
<http://www.clr.uwa.edu.au> Email [fmengler@agric.uwa.edu.au](mailto:fmengler@agric.uwa.edu.au)

## Abstract

The high strength of some regolith types can limit the growth of replanted jarrah forest following bauxite mining in southwestern Australia. Ripping mine floors to a depth of 1.5m can successfully alleviate high strength zones and improve root exploration of some substrates; however, this practice is expensive. An understanding of the spatial distribution of regolith strength enables a mining company to conduct second-pass ripping in areas most in need of amelioration while leaving softer, structured regolith un-ripped. We developed regolith strength maps, based on real-time measurement of the hydraulic fluid pressure in the tilt cylinders of Komatsu 475 and Caterpillar D11R bulldozers with standard tip, single shank deep-ripping tines. The maps show positions of high-, medium- and low-strength zones in the floors of former opencast bauxite mines. A data logger recorded tine depth, vehicle speed and pressure sensor measurements every 2 seconds. Location data were recorded with a GPS. The spatial variation of regolith strength was mapped using ARCMAP 8.3 GIS software. Evaluation of the maps using excavated regolith profiles showed a reliable relationship between bulldozer-mapped regolith strength and mean cone index. The mining company is now provided with maps showing the spatial distribution of regolith strength.

## Key Words

Precision, tillage, hardness, fracture, rippability, rehabilitation.

## Introduction

### *Mine floor regolith*

Successful jarrah forest rehabilitation after bauxite mining depends on the properties of mine floor regolith. Together with replaced topsoil and a second layer referred to as overburden, mine floor regolith is part of the reconstructed soil profile in which re-established vegetation grows. Bauxite mine floors in the Darling Range, Western Australia contain a diverse range of regolith materials developed from the lower mottled zone, pallid zone or saprolite part of the profile (McArthur 1991). Mine floor regolith has a complex distribution of physical properties that may impede the growth of plant roots, leading to patchy regrowth. Many regolith types have inherent physical properties that allow adequate root exploration and plant reestablishment without the need for additional manipulation by tillage. These materials often have pre-existing root channels (Dell *et al.* 1983), adequate structure, stable aggregates and a capacity to store plant-available water. Indeed it is often counter-productive to rip these regolith types as fragile macropore networks and other structures can be destroyed by ripping. The majority of mine floor regolith however, does require ripping to induce macrostructure and alleviate high strength and high bulk density. Ripping also alleviates traffic pans caused by mining vehicle-induced compaction (Croton and Watson 1987). Ripping fractures dense and/or hard zones and induces structure within the regolith; it increases the volume of friable soil accessible to plant roots and thus improves the performance of re-established ecosystems.

### *Bauxite mine rehabilitation and ripping*

Alcoa World Alumina Australia (Alcoa) operates two lateritic bauxite mines at Willowdale and Huntly in the Darling Range of southwestern Western Australia. The Darling Range is covered by indigenous eucalypt forest, dominated by jarrah (*Eucalyptus marginata*). Mining currently removes and restores about 550ha of this forest per year. The objective of restoration is to return a jarrah forest ecosystem that retains all of the pre-mining land uses including water and timber production, conservation and recreation. A detailed description of the mining and restoration processes is found in Gardner (2001). Alcoa has been ripping mine floor regolith and improving ripping techniques since 1969. Ripping is currently conducted in two stages. Stage one known as 'pre-ripping', is ripping in straight lines with a straight tine across mine floors. Next the pre-ripped floors are graded, and topsoil and overburden are deposited by scrapers. Stage two is ripping along the contour with a winged tine to mix seed, topsoil and overburden with the previously-ripped mine floor.

### *Aims of this research*

It is current practice to conduct deep ripping on all mine floors in the same manner, ignoring the spatial distribution of different regolith materials. Past experience has shown that it is difficult to rip an entire mine floor to a constant depth of 1.5m because regolith strength varies greatly and a bulldozer operator may raise the tine to rip through hard ground. Alcoa is committed to ripping over 80% of the mine floor to a depth of 1.5m to provide an adequate root zone in the soil. Mapping the distribution of mine floor regolith strength will provide Alcoa with a tool to locate and understand the causes of shallow ripping, adding greater sophistication to its ripping practices. Furthermore, it may be possible to optimise ripping techniques for each regolith material, in much the same way as farmers using precision agriculture technology apply inputs based on soil and yield maps (Booltink *et al.* 2001). Our investigation aimed to answer the following questions:

- Can an instrumented bulldozer map the spatial distribution of regolith strength in mine floors?
- Is bulldozer-measured strength related to the pedology/material characteristics of the regolith?
- Can regolith strength be used as a tool to map the distribution of regolith materials?

### **Methods**

#### *Bulldozer instrumentation*

One Komatsu 475 and two Caterpillar D11R bulldozers were each equipped with an onboard computer, GPS, pressure and depth sensors and power supply (Figure 1a). Tine depth was measured by an angle encoder and pivot rod attached to the lift cylinder of the ripper. At constant working depth the penetration force required to rupture the mine floor can be approximated by the hydraulic pressure within the tilt cylinders of the ripper (Figure 1a). We measured the fluctuation of hydraulic pressure in the ripper tilt cylinders with Trafag (0-255 bar) industrial pressure transducers.

Latitude, longitude and apparent vehicle speed were determined with a Farmscan GPS 3002 global positioning system (supplying 2-5m accuracy 95% of the time, maximum error 10m). Output signals from the sensors and GPS were logged using a Farmscan Canlink 3000 precision farming computer and customized data acquisition software. All measurements occurred during the pre-ripping operation and henceforth, reference to 'ripping' in this paper means pre-ripping. The instrumented rippers were pulled by bulldozers to produce parallel lines of ripping identified as lines 1, 2, 3, and 4 etc. in Figure 1b.

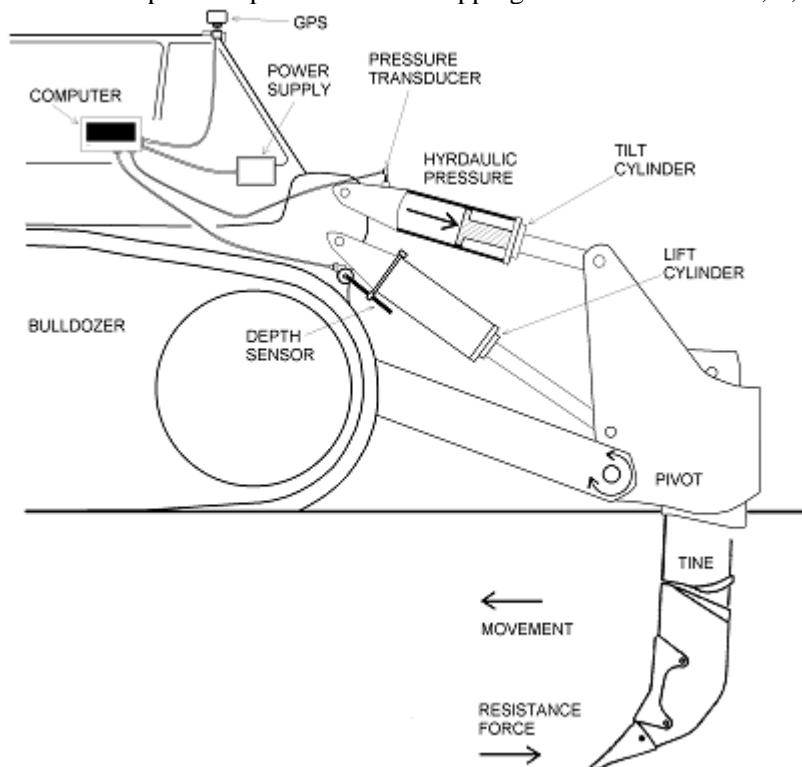


**Figure 1. (a.) The instruments and equipment installed on the bulldozers to measure ripping pressure, tine depth, location and bulldozer speed.**

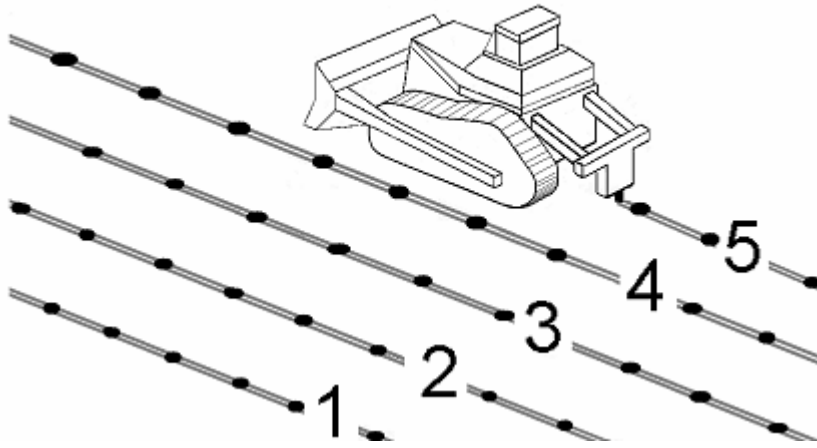


**Figure 1. (b.) Pre-ripping lines were spaced approximately 2m apart. Ripping data points (shown as black circles) were spaced approximately 2m apart.**

*Data processing*

Data were downloaded daily, processed using Computronics Farmscan software and imported into an ESRI ARCMAP 8.3 GIS as point shapefiles. The processed datasets contained the following information:

- position (AMG eastings and northings)
- hydraulic pressure of ripper tilt cylinders (bar)
- depth of tine (metres)
- speed of bulldozer (metres per second)

*Data interpolation*

All datasets contained thousands of points. Summary statistics for three ripped sites are shown in Table 1. To produce a continuous surface map and to differentiate between noise and information we used an inverse distance weighted (IDW) spatial interpolation method. Although IDW does not have the statistical advantages of kriging, it is less laborious and as accurate as kriging for large intensive datasets (Kravchenko 2003). We assumed that fluctuations in speed, hydraulic pressure and depth of tine reflected the local variation in regolith strength; and that this spatial variation could be captured through the local neighbourhood. Spatial variation in regolith properties at a scale of less than 10m is common. Johnston (1987) found that deep clayey regolith in southwest WA showed marked heterogeneity over horizontal and vertical distances of only a few metres. To account for this small-scale variation we used a fixed search radius of 5m and a power of 2 to interpolate data into 2 x 2m IDW grids using ArcMap 8.3 Spatial Analyst software.

**Table 1. Summary statistics for raw ripping data.**

Pit	variable	mean	median	minimum	maximum	std. dev.	coef. var.	skewness	kurtosis
Chipala 9 (n=4659)	pressure (bar)	14.5	10.0	1.20	248.4	21.3	1.47	5.31	35.6
	depth (m)	1.50	1.54	0.20	1.83	0.25	0.17	-3.54	13.7
	speed (ms <sup>-1</sup> )	0.69	0.76	0.01	2.11	0.34	0.49	-0.30	0.14
Mullian 3 (n=8718)	pressure (bar)	15.0	10.0	1.20	244.7	20.3	1.35	4.80	29.2
	depth (m)	1.58	1.58	0.31	1.96	0.16	0.10	-3.22	17.1
	speed (ms <sup>-1</sup> )	0.73	0.83	0.02	2.05	0.28	0.39	-0.94	0.63
Thylacine 7 (n=15400)	pressure (bar)	21.4	10.0	1.00	253.0	38.0	1.78	3.95	17.3
	depth (m)	1.58	1.61	0.31	1.99	0.19	0.12	-2.60	10.7
	speed (ms <sup>-1</sup> )	0.79	0.71	0.01	2.12	0.39	0.50	1.29	1.21

*Map classification*

We classified each IDW map into four classes, grouping values based on least-variance within classes and maximum variance between the classes (Jenks 1977). Break values between classes of the same variable at different study sites did not coincide so we developed common break values to allow comparison of maps

between different sites. Using data summarised in Table 2 (approximately 10ha of ripping) we determined the first (lowest) break value for each ripping variable by averaging the median over the three sites as follows: ripping pressure (13 bar), tine depth (1.5m) and bulldozer speed (0.8m/s). Discussions with bulldozer operators confirmed that these values did indeed mark the upper limit of low ripping draught conditions. Subsequent break values divided the remaining upper half of the data into equal intervals (i.e. between quantiles:  $q_{0.5}$  and  $q_{0.66}$ ;  $q_{0.66}$  and  $q_{0.83}$ ; and  $q_{0.83}$  and  $q_{1.0}$  of the distribution). Manual reclassification produced four-colour maps for each of the variables: ripping pressure, tine depth and bulldozer speed. Blue classes on the maps represent low-draught or normal operating conditions; green, yellow and red classes indicate moderate, high and extreme draught respectively.

**Table 2. Summary statistics for IDW-interpolated ripping data.**

Study site	Ripping pressure (bar)			Tine depth (m)			Bulldozer speed ( $\text{ms}^{-1}$ )		
	mean	std. dev.	median	mean	std. dev.	median	mean	std. dev.	median
Chipala 9	15.3	11.2	12.0	1.50	0.15	1.50	0.78	0.17	0.81
Mullian 3	13.5	9.6	12.6	1.57	0.11	1.57	0.79	0.15	0.86
Thylacine 7	20.9	9.6	14.6	1.47	0.19	1.48	0.80	0.19	0.71

### Sample trenches

Two ripped sites were chosen for detailed field evaluation of regolith properties, and to relate these properties to the bulldozer-mapped ripping variables. Mullian 3 and Chipala 9 sites are both located at the Huntly mine site. Pedological description of regolith material was made from 20 trenches excavated at Mullian 3 and 16 trenches at Chipala 9. Excavated trenches were 5m long, 3m wide and 2.5m deep with stepped 1m-wide safety benches. A regolith classification system was developed to describe the mine floor regolith materials and a simplified version of this is shown in Table 3.

**Table 3. Simplified classification and properties of Darling Range bauxite mine floor regolith.**

Regolith Material	Texture (by hand)	Colour (Munsell)	Coarse Fragments (%)	Quartz (%)	Pedality			Bulk Density ( $\text{g/cm}^3$ )	P.A.W.* ( $\text{m}^3/\text{m}^3$ )
					Grade	Type	Size		
Topsoil	loamy sand to sandy loam	10YR3/4	40 – 60	30 – 50	apedal	granular	single grain	1.1	< 0.10
Overburden	loamy sand to sandy loam	10YR6/8 to 2.5Y6/8	40 – 60	30 – 50	apedal	granular	single grain	1.1	< 0.10
Mottled zone	sandy loam to sandy clay	10YR5/6 to 2.5Y7/6	< 50	30 – 60	weak to moderate	subangular to blocky lenticular	1cm to 10cm	1.8	0.11 to 0.12
Pallid zone	silty loam to silty clay	10YR7/3 to 5Y8/1	< 30	< 30	moderate to strong	angular blocky	2cm to 10cm	1.7	0.15 to 0.17
Sandy ferricrete (cemented)	coarse sand to loamy sand	7.5YR5/6 to 10YR5/8	> 50	30 - 60	apedal cemented	duripan	single grain to cemented	2.0	$\leq$ 0.10
Sandy bauxite (friable)	coarse sand to loamy sand	7.5YR5/6 to 10YR5/8	< 50	30 - 60	apedal	granular	single grain	1.6	$\leq$ 0.10
Granitic saprolite	sand to sandy clay loam	10YR5/6	50 - 80	< 30	apedal to weak	granular to subangular blocky	single grain to 5 cm	1.7	0.10
Doleritic saprolite	sandy loam to clay loam	5YR4/6 to 5YR5/8	50 - 80	< 10	weak to moderate	subangular to angular blocky	2cm to 10cm	1.7	0.12

\*Volumetric plant available waterholding capacity between field capacity, pF2 (-10kPa) and wilting point, pF4.2 (-1500kPa)

### Confined compressive strength (cone penetrometer) measurements

The confined compressive strength of regolith in each sample trench was measured with a Rimik CP20 Ultrasonic penetrometer with a cone diameter of 12.8mm (Davidson, 1965). We used the average of three replicates of unripped regolith, each returning 5 measurements from a 50-60cm depth range on the first safety bench (approx 1m deep) of each trench. This is where: (1) penetration resistance most reliably represented that of intact (non-ripped) material and (2) the depth of measurement was similar to the depth of tine during ripping (1.5m). All measurements from both sites were taken on the same day approximately 30 hours after rainfall. Extremely hard (impenetrable) and gravely regolith was omitted from the dataset.

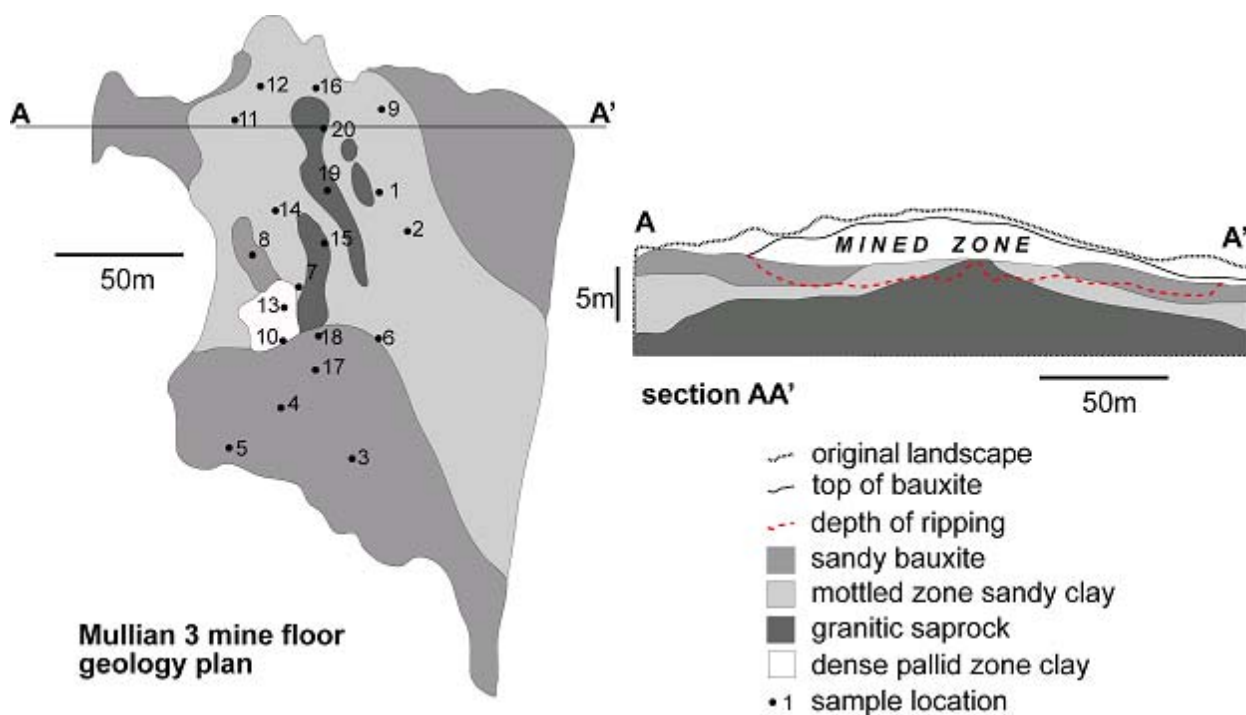


**Figure 2. Plan and section of Mullian 3 mine floor regolith based on field mapping and interpretation of borehole data.**

#### *Description of Mullian 3 and Chipala 9 study sites*

The mine floor of Mullian 3 is represented by plan and section views in Figure 2. Mullian 3 is characterised by outcropping and subcropping granitic saprock at the centre of the pit. Friable sandy bauxite occurs in the northeast and northwest corners and along the southern edge of the pit, extending towards the centre. The majority of mine floor regolith is composed of quartz-rich, sandy clay of the mottled zone (Table 3) similar to the material shown in Figure 2. Moderate amounts of dense, pallid zone clay occur in a discrete area west of the centre of the pit. Clay bodies such as these are often derived from the weathering of dolerite or low-quartz felsic rocks.

The mine floor of Chipala 9 is represented by plan and section views in Figure 3. Chipala 9 has mine floor regolith derived from both granitic and doleritic parent materials. Yellow-brown, sandy clay of the mottled zone covered most of the area. When compared with Mullian 3, iron oxide occurred in greater abundance in the regolith of Chipala 9. Weathered dolerite corestones occurred in trenches 5 and 9. Dense pallid zone clay occurred in trenches 8, 12 and 14; this material may be a product of the weathering of dolerite or a low-quartz felsic rock. A residual body of sandy bauxite occupied a 15 to 20m wide zone from trench 10 to trench 11. Discrete pods (1-2m) of sandy ferricrete occurred within the sandy bauxite zone and elsewhere in the sandy clay material of the mottled zone, often associated with ironstone gravels.

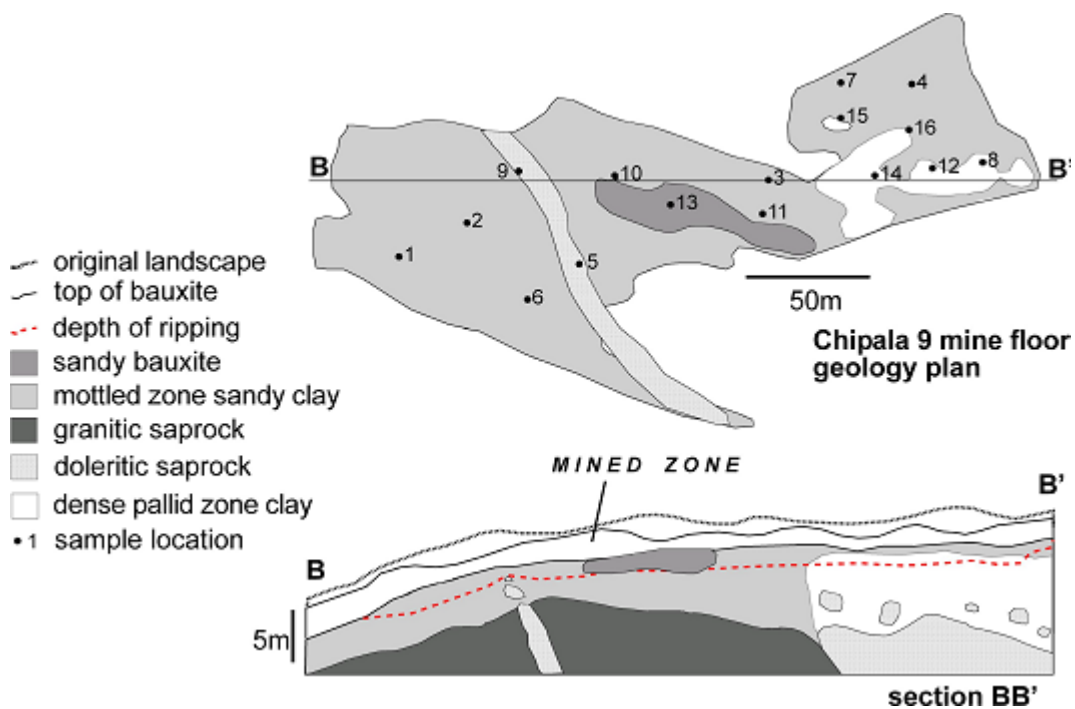


**Figure 3. Plan and section of Chipala 9 mine floor regolith based on field mapping and interpretation of borehole data.**

## Results

### *Relationship between ripping variables*

The three variables: depth, pressure and speed were interrelated. Pressure generally had an inverse relationship with both tine depth and bulldozer speed. Hard regolith increased draft on the operating tine, decreasing bulldozer speed; at the same time, an automatic hydraulic control valve adjusted to the increased draft by raising pressure in the tilt cylinder. Wishing to maintain forward motion, the operator manually compensated for the reduction in speed by raising the tine before track-slip occurred. High pressure was often associated with low bulldozer speed and low tine depth. Conversely, softer regolith offered less resistance to the passage of the tine resulting in low pressure, higher bulldozer speed and greater tine depth.

### *Discussion of Mullian 3 ripping variable maps*

Some spatial patterns within maps in Figure 4 can be explained by the nature of the mine floor regolith (Figure 2). Parts of the high strength central granitic saprock zone resulted in low tine depth shown by the red and yellow zones in Figure 4b, especially around sample trench 19. Figure 4c shows that ripping pressure mapped the location of hard granitic saprock around sample trenches 15, 19 and 20. Residual sandy bauxite and sandy mottled zone regolith were mapped as blue zones in both Figures 4b & c. Lower ripping depths shown as yellow and green zones in the southeast and northeast parts of the pit in Figure 4b are probably due to the bulldozer operator raising the tine to turn at the ends of each ripline.

To correctly interpret Figure 4d the red and yellow sections at the edges of the map must be ignored. These artefacts are not caused by the regolith. Speed was low because the bulldozer was close to the end of the riplines. Bulldozer speed was relatively constant through the central zone of high-strength, granite saprock that displays as low depth and high pressure in Figures 4b & c respectively. We expected this material to impede the bulldozer causing low speed. On inspection the majority of saprock boulders were scraped rather than fractured indicating that the tine deflected the saprock but was not impeded by it, allowing speed to remain constant. Of interest in Figure 4d are linear sets of weak to moderately spatially persistent low-speed values in the 0.5 to 0.8m/s range (green and yellow zones), for example the line extending through trenches 6, 15 and 14. The linear trends do not coincide with ripping direction so they are not an artefact of the data logging procedure. These “lineaments” have a northwesterly trend which is the dominant structural trend within the Darling Range bedrock (Hickman *et al.* 1992).

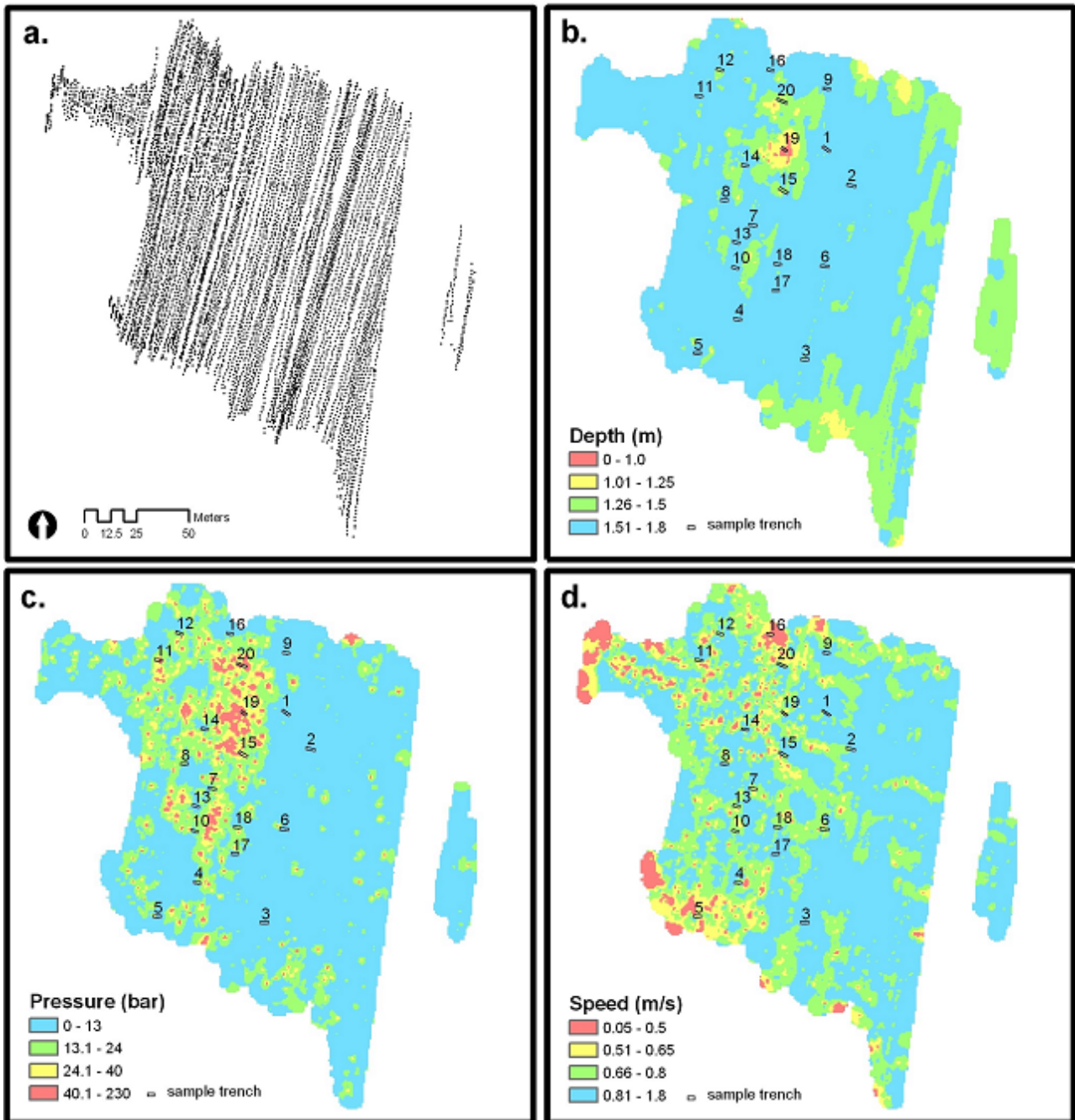


**Figure 4.** Maps of Mullian 3 bauxite pit showing data points (a), tine depth (b), ripping pressure (c) and bulldozer speed (d). Blue areas on the maps represent low-draught or normal operating conditions; green, yellow and red areas indicate moderate, high and extreme draught conditions respectively.

#### *Discussion of Chipala 9 ripping variable maps*

High tine depth (blue class in Figure 5b) was recorded in much of the mottled zone sandy clay of Chipala 9 (Figure 3). As with Mullian 3, low depth values were recorded at the ends of many riplines and these should be ignored. The southwest part of Figure 5c shows low ripping pressure associated with mottled zone sandy clay. Discrete patches (~5m in size) of high and extreme pressure (yellow and red classes) caused by pods of hard ferricrete occurred within sandy bauxite near trenches 10, 13 and 11 (Figure 5c). Similar patches near trenches 5 and 9 were associated with hard dolerite corestones. Dense pallid zone clay at the surface and in trenches 8, 12, 14, 15 and 16 was associated with sporadic high pressure bullseyes. Ripping pressure did not clearly define the zone of doleritic saprock trending southwest from trench 9 to beyond trench 5 because this material had both hard and soft zones caused by highly variable extent of weathering.

Low to moderate bulldozer speed was associated with the dense pallid zone clay around trenches 8, 12, 14, 15 and 16 (Figure 5d). Sporadic elliptically-shaped patches of low bulldozer speed, aligned in the direction

of ripping were associated with cemented zones within the sandy bauxite near trenches 10, 13 and 11. Mottled zone sandy clay around trenches 1, 2, 3, 4, 6 and 7 resulted in areas of both low and moderate bulldozer speed. Complexly-distributed iron oxide cementing agents may have produced within-material variations of both ripping pressure and bulldozer speed.

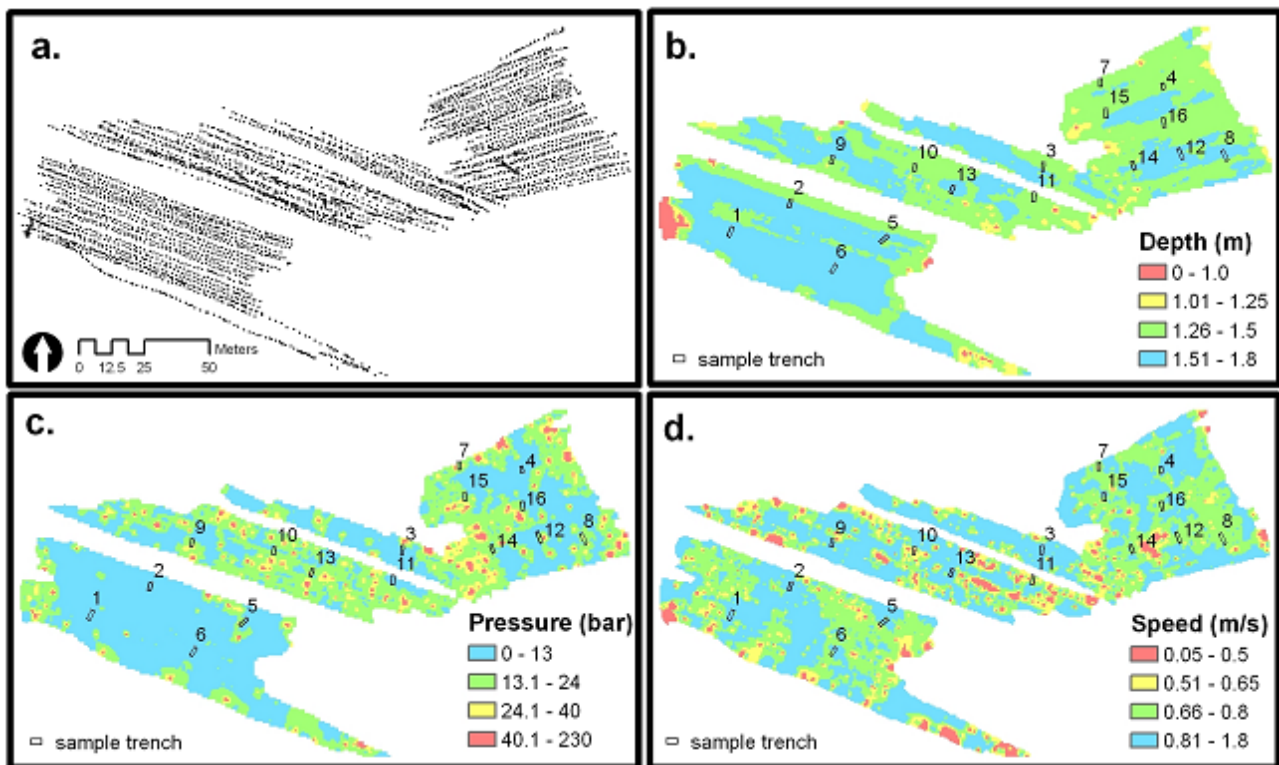


**Figure 5.** Maps of Chipala 9 bauxite pit showing data points (a), tine depth (b), ripping pressure (c) and bulldozer speed (d). Blue areas on the maps represent low-draught or normal operating conditions; green, yellow and red areas indicate moderate, high and extreme draught conditions respectively.

#### *Calibration of bulldozer-measured regolith strength*

Penetrometer pressure (cone index) indicates the force needed to displace particles at the tip against the retaining force of the overburden soil (Bradford *et al.* 1971). Penetration resistance is mainly a function of interparticle binding forces and the friction between moving particles (Bennie 1991). The resistance to a moving tine (Figure 1a) is also *inter alia* a function of interparticle binding forces and friction. Regolith strength and pedology were assessed on all trench faces by prising out peds of material with a hoe pick and a blunt knife. Pressure was more closely related to regolith strength when measured in this semiquantitative manner than the other two variables. We then compared ripping pressure to the mean cone index of representative regolith material from each of the 36 sample trenches. To enable this comparison each trench was categorised based on its colour (classification) in the ripping pressure maps (Figures 4c & 5c) and assigned one of six strength categories (Table 4).

**Table 4.** Categories of regolith strength at each sample trench according to the ripping pressure variable.

Colours at trench location Figs. 4c & 5c)	Regolith strength category	Mullian 3 trench nos.	Chipala 9 trench nos.
blue	1	1,2,3,6,9,13	1,2,4,6,11
blue/green	2	4,5,14,16,17	3,5,10,14
green	3	7,8,12,18	8,13,15,16
green/yellow	4	10	7,12
yellow	5	11,15	9
red	6	19,20	

The strength of regolith material as measured by cone penetrometer showed a systematic positive relationship to classified and categorised bulldozer-measured strength (Figure 6).

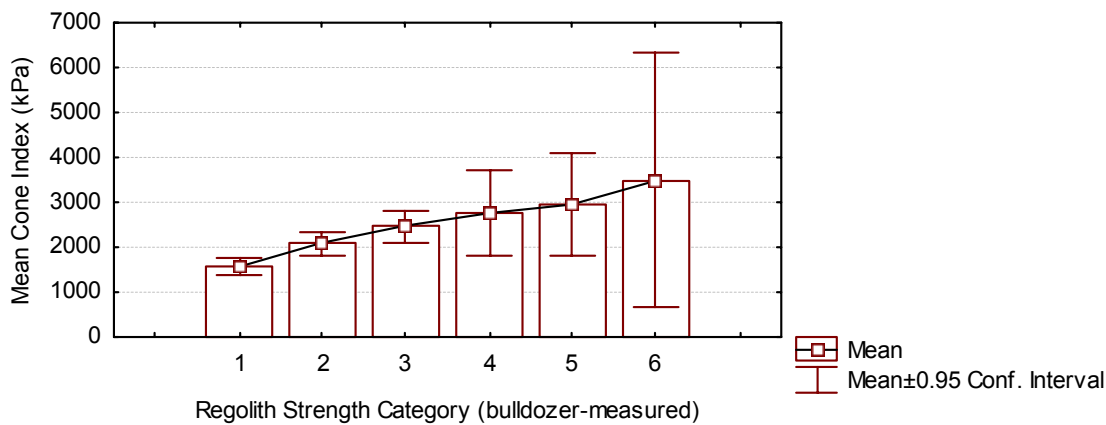


**Figure 6. The relationship between mean cone index and regolith strength category (bulldozer-measured).**

### Conclusions

The distribution of regolith strength can be mapped by an instrumented bulldozer. Tine depth distinguished large (>10m) bodies of extremely strong material like saprock from other mine floor materials but was the least sensitive indicator of regolith variability. Bulldozer speed maps show patterns that may reflect variation in the fabric of regolith that has been inherited from parent materials, further work is necessary to evaluate this. Out of three ripping variables, pressure was most closely related to regolith strength. Regolith strength was highly variable spatially and this variation was at least partly controlled by geological structure. Sandy clay material from the mottled zone generally fell within the lowest regolith strength category. Silty clay from the pallid zone produced some high strength readings although these were not uniform throughout the material. The concentration and distribution of cementing agents including iron oxide and gibbsite within regolith materials exerted a significant control on bulldozer-mapped strength. Classified and categorised bulldozer-measured strength had a systematic positive relationship to penetration resistance (mean cone index). An index that combines the three ripping variables: depth, pressure and speed may be more predictive of the spatial variability of the regolith and is the subject of ongoing research.

### Acknowledgements

This research was funded by the ARC and Alcoa as part of Linkage Project LP0214954.

### References

- Booltink HWG, van Alphen BJ, Batchelor WD, Paz, JO, Stoorvogel JJ and Vargas R (2001) Tools for optimizing management of spatially-variable fields. *Agricultural Systems* **70**, 445-476.
- Bradford JM, Farrell DA and Larson WE (1971) Effect of soil overburden pressure on penetration of fine metal probes. *Soil Science of America Proceedings* **35**, 12-15.
- Croton JT and Watson GD (1987) Mining related compaction - a case study in the Darling Range, Western Australia. *Alcoa of Australia Ltd. Environmental Research Bulletin* **14**.
- Davidson DT (1965) Penetrometer measurement. In 'Methods of soil analysis, Part 1'. Agronomy Series, No. 9. pp. 472-484. (Soil Science Society of America: Madison, WI).
- Dell B, Bartle JR and Tacey WH (1983) Root occupation and root channels of jarrah forest subsoils. *Australian Journal of Botany* **31**, 615-627.
- Gardner JH (2001) Rehabilitating mines to meet land use objectives: bauxite mining in the jarrah forest of Western Australia. *Unasylva* **207**, 3-8.
- Hickman AH, Smurthwaite AJ, Brown IM and Davy R. (1992) Bauxite mineralization in the Darling Range, Western Australia. *Geological Survey of Western Australia Report* **33**, 10-11.
- Jenks, G. (1977). Optimal Data Classification for Choropleth Maps. Occasional Paper 2, Department of Geography, University of Kansas.
- Johnston, CD (1987) Preferred water flow and localised recharge in a variable regolith. *Journal of Hydrology* **94**, 67-88.
- Kravchenko, AN, (2003) Influence of spatial structure on accuracy of interpolation methods. *Soil Sci. Soc. Am. J.* **67**, 1564-1571.
- McArthur WM (1991) Reference soils of south-western Australia. W.A. Dept. Agriculture & Aust. Soc. Soil Sci. W.A. Branch) p21.